HHS Public Access

Author manuscript

Cell Rep. Author manuscript; available in PMC 2017 June 23.

Published in final edited form as:

Cell Rep. 2017 April 18; 19(3): 617–629. doi:10.1016/j.celrep.2017.03.070.

Liberated PKA catalytic subunits associate with the membrane via myristoylation to preferentially phosphorylate membrane substrates

Shane E. Tillo[*], **Wei-Hong Xiong**[*], **Maho Takahashi**, **Sheng Miao**, **Adriana L. Andrade**, **Dale A. Fortin**, **Guang Yang**, **Maozhen Qin**, **Barbara F. Smoody**, **Philip J. S. Stork**, and **Haining Zhong**

Vollum Institute, Oregon Health & Science University, Portland, Oregon 97239

SUMMARY

Protein kinase A (PKA) has diverse functions in neurons. At rest, the subcellular localization of PKA is controlled by A-kinase anchoring proteins (AKAPs). However, the dynamics of PKA upon activation remain poorly understood. Here we report that elevation of cAMP in neuronal dendrites causes a significant percentage of the PKA catalytic subunit (PKA-C) molecules to be released from the regulatory subunit (PKA-R). Liberated PKA-C becomes associated with the membrane via N-terminal myristoylation. This membrane association does not require the interaction between PKA-R and AKAPs. It slows the mobility of PKA-C and enriches kinase activity on the membrane. Membrane-residing PKA substrates are preferentially phosphorylated compared to cytosolic substrates. Finally, the myristoylation of PKA-C is critical for normal synaptic function and plasticity. We propose that activation-dependent association of PKA-C renders the membrane a unique PKA-signaling compartment. Constrained mobility of PKA-C may synergize with AKAP anchoring to determine specific PKA function in neurons.

INTRODUCTION

Cyclic adenosine monophosphate (cAMP)-dependent kinase, or protein kinase A (PKA) regulates diverse critical functions in neurons, including neuronal excitability, protein trafficking, protein degradation, gene transcription, and synaptic plasticity. PKA is a tetrameric protein consisting of two regulatory subunits (PKA-Rs) and two catalytic subunits (PKA-Cs) (Francis and Corbin, 1994; Johnson et al., 2001). In the inactive state, each PKA-

Correspondence should be addressed to H.Z. zhong@ohsu.edu.

[*]These authors contributed equally to the work

Lead Contact: Dr. Haining Zhong, Vollum Institute, Oregon Health & Science University, 3181 SW Sam Jackson Park Road, L474, Portland, Oregon 97239, U.S.A., (503) 494-5089/ zhong@ohsu.edu

SUPPLEMENTAL INFORMATION

Supplemental Information includes seven figures and supplemental experimental procedures.

AUTHOR CONTRIBUTIONS

H.Z. conceived the study. S.E.T., W.H., P.J.S.S. and H.Z. designed the experiments. S.E.T., W.H., M.T., S.M., A.L.A., D.A.F. and H.Z. performed the experiments with indispensable assistance from G.Y., M.Q. and B.F.S. S.E.T., W.H., M.T. and H.Z. analyzed the data. S.E.T., P.J.S.S. and H.Z. wrote the paper.

The authors declare that there is no conflict of interest.

R binds to and inhibits a single PKA-C. Binding of cAMP to PKA-R releases and disinhibits PKA-C. Liberated PKA-C then moves to phosphorylate its diverse set of substrates.

When cAMP concentrations are low, most PKA in neurons is anchored. PKA-R, especially the type II isoform, binds to scaffold proteins called A-kinase anchoring proteins, or AKAPs (Lohmann et al., 1984; Scott and Pawson, 2009; Wong and Scott, 2004). Over 50 AKAPs have been identified and many of them are expressed in neurons. They recruit holo-PKA to distinct subcellular compartments near relevant signaling proteins and/or substrates. Disrupting the binding of AKAP to PKA-R can interfere with PKA phosphorylation of substrates (Colledge et al., 2000; Davare et al., 2001; Lu et al., 2007; Lu et al., 2008; Smith et al., 2013). AKAP-anchoring of PKA is thought to be a major mechanism by which PKA achieves its specificity among its substrates (Scott and Pawson, 2009; Wong and Scott, 2004).

Less is known about the dynamics of PKA in neurons following PKA activation. Several studies have suggested that PKA-C may exhibit kinase activity without leaving PKA-R (Johnson et al., 1993; Smith et al., 2013; Yang et al., 1995). However, the vast majority of the literature indicates that PKA-C is released from the AKAP/PKA-R complex during physiological elevations of cAMP concentration (Beavo et al., 1974a; Buxton and Brunton, 1983; Francis and Corbin, 1994; Johnson et al., 2001; Turnham and Scott, 2016). Liberated PKA-C is generally viewed as a cytosolic protein because of its high solubility (Johnson et al., 2001). However, free-moving cytosolic proteins diffuse rapidly with a diffusion coefficient of ~50 $\mu m^2/s$ (Bloodgood and Sabatini, 2005; Swaminathan et al., 1997) and can travel micrometers or farther within the time course of PKA signaling events (~ seconds to minutes) (Brooker, 1973; Dunn et al., 2006; Gorbunova and Spitzer, 2002; Ni et al., 2010; Zhou and Adams, 1997). Because many neuronal compartments, such as dendritic spines, are small (~ 1 μm), the mobility of a freely diffusing PKA-C would be expected to break down the spatial specificity established by AKAPs. Additional mechanisms constraining the movement of PKA-C may therefore be required to sustain PKA specificity.

Here, we show that, a significant fraction of PKA-C molecules is freed from the AKAP/PKA-R complex upon activation in hippocampal pyramidal neurons in slices. Liberated PKA-C exhibits mobility considerably slower than freely-diffusing cytosolic proteins of comparable size and instead its mobility is similar to membrane-associated proteins. This low mobility is independent of AKAP anchoring of PKA-R and is, in part, mediated by an N-terminal myristoylation modification on PKA-C. PKA-C, while distributed within the cytosol in living neurons at rest, becomes associated with the membrane upon activation in a myristoylation-dependent manner. PKA substrates residing on the membrane were preferentially phosphorylated over the same substrates in the cytosol. Myristoylation of PKA-C appears to be required for normal PKA regulation of synaptic function and plasticity. We have thereby established a physiological function of PKA myristoylation and provided evidence for a mechanism that may synergize with AKAPs to govern the signaling specificity of PKA.

RESULTS

PKA-C dissociates from the PKA-R/AKAP complex in neurons upon activation

Two experiments were performed to visualize whether PKA-C can be freed from the PKA-R/AKAP complex upon activation *in situ* in neuronal dendrites.

First, we used two-photon fluorescence life time imaging microscopy (2pFLIM) (Yasuda et al., 2006) to quantify Förster resonance energy transfer (FRET) between C-terminally EGFP tagged PKA-C alpha isoform (PKA-C-EGFP) and C-terminally sREACh-tagged PKA-RIIβ (PKA-RIIβ-sREACh) in rat organotypic cultured hippocampal slices (Figure 1A). sREACh is a low-irradiating YFP (Murakoshi et al., 2008). 2pFLIM measures the fluorescence lifetime, i.e., the average time elapsed between fluorophore excitation and photon emission of the donor fluorophore, which is shortened when FRET occurs. Among its advantages in quantifying FRET, 2pFLIM allows for the determination of the binding ratio between PKA-C-EGFP and PKA-R-sREACh. If PKA-C leaves PKA-R upon activation, its binding ratio, as quantified using 2pFLIM, would decrease (Figure 1A).

At rest, the binding ratio was 27 ± 2 % for PKA-C-EGFP. This low binding ratio may be due to abundant endogenous PKA-R (~0.2–0.7 μM in many cell types) (Flockhart and Corbin, 1982; Francis and Corbin, 1994) and incomplete folding of sREACh (Murakoshi et al., 2008). Application of 20 μM norepinephrine, which is in the mid-range of what neurons see with endogenous releases (Courtney and Ford, 2014), decreased the binding ratio by 12 ± 3% in neuronal dendrites (Figure 1B and 1C, $p < 0.01$ at peak, c.f. baseline), suggesting that a small but significant portion of PKA-C-EGFP dissociated from PKA-RIIβ-sREACh. The binding ratio was decreased by ~70% from baseline with stronger stimulation using forskolin and IBMX (Figure 1B and 1C). Co-immunoprecipitation (co-IP) experiments in HEK 293 cells showed that 55 ± 7% of PKA-C-mCherry remained bound to PKA-RIIβ and AKAP5-EGFP upon stimulation with forskolin and IBMX (Figure S1), suggesting that activation of PKA in HEK cells is less strong than in neurons. The remaining binding was nearly completely abolished (6 ± 3% remained bound) by adding the cAMP analog Sp-8-pCPT-cAMP (5 μM) to the IP reaction. Thus, forskolin and IBMX did not elevate intracellular cAMP levels enough to cause complete dissociation. Overall, these results indicate that a portion of PKA-C is liberated from PKA-R upon physiological cAMP elevation.

Second, we monitored the subcellular dynamics of PKA-C-EGFP co-expressed with untagged PKA-RIIβ, or PKA-RIIβ-EGFP alone in separate experiments with reference to a red cytosolic marker (mCherry). The distribution of expressed PKA-C and PKA-RIIβ reflect that of the endogenous PKA proteins (Parisiadou et al., 2014; Zhong et al., 2009). PKA-C-EGFP and PKA-RIIβ-EGFP exhibited similar subcellular distributions under basal conditions: higher concentrations of PKA subunits were found in dendritic shafts than in adjacent spines (Figure 1D and S2). This distribution was quantified by using the spine enrichment index (SEI) (Figure 1E) (Zhong et al., 2009):

$$\mathrm{SEI}=\log_2([\mathrm{Green}/\mathrm{Red}]_{\mathrm{spine}}/[\mathrm{Green}/\mathrm{Red}]_{\mathrm{dendrite}}).$$

A positive SEI implies protein enrichment in the spine; whereas a negative SEI indicates exclusion from the spine. Upon stimulation with norepinephrine, PKA-C-EGFP translocated to dendritic spines (SEI = −0.84 ± 0.07 at rest, and −0.31 ± 0.06 at 6 min after stimulation, $p < 0.001$) (Figure 1D, 1E and S2). Forskolin and IBMX induced a further translocation (SEI = 0.71 ± 0.03, $p < 0.001$, c.f. baseline). In contrast, the distribution of PKA-RIIβ-EGFP did not change under the same conditions (SEI = −0.92 ± 0.07 at rest, −0.97 ± 0.07 with norepinephrine, −1.09 ± 0.07 with forskolin and IBMX; $p < 0.001$ c.f. PKA-C-EGFP after stimulation) (Figure 1D and 1E). The portion of PKA-C translocating to spines must have dissociated from the PKA-R/AKAP complex.

PKA-C has significantly lower mobility than cytosolic proteins

We next examined the mobility of liberated PKA-C. CA1 neurons were transfected with photoactivatable GFP (paGFP) (Patterson and Lippincott-Schwartz, 2002) tagged PKA-C (PKA-C-paGFP), PKA-RIIβ, and mCherry. We used focal two-photon photoactivation to irreversibly convert paGFP to the bright state and monitored the resulting fluorescence decay over time, as an assay for PKA-C mobility (Figure 2A and 2B) (Bloodgood and Sabatini, 2005; Gray et al., 2006). To preferentially examine liberated PKA-C, we focused on spines to take advantage of their low basal PKA-C concentration (Figure 1D and 1E). The time constant of fluorescence decay at the spine (i.e., the spine-residence time) is linearly inversely proportional to the diffusion coefficient of a protein (Bloodgood and Sabatini, 2005). In the presence of norepinephrine, PKA-C-paGFP exhibited a spine-residence time about 8-fold longer than that of cytosolic paGFP (τ = 2.11 ± 0.06 s for PKA-C-paGFP and 0.26 ± 0.01 s for paGFP; $p < 0.001$; Figure 2C), indicating that PKA-C has a mobility much lower than that of free-diffusing cytosolic proteins. Further increase in intracellular cAMP concentration with forskolin and IBMX did not make PKA-C-paGFP diffuse more rapidly (τ = 2.34 ± 0.08 s), suggesting that the low mobility was not due to residual binding with PKA-R at lower cAMP concentrations.

The low mobility of PKA-C cannot be explained by the larger size of PKA-C-paGFP (67 kD) compared to paGFP (27kD). Based on size alone (the diffusion coefficient for globular proteins increases in proportion to the cubic root of the molecular weight, (Papadopoulos et al., 2000)), PKA-C-paGFP would be expected to diffuse ~35% more slowly than paGFP, corresponding to a spine-residence time of ~0.4 s, which is far less than what was observed. Indeed, when we used fluorescence recovery after photobleaching (FRAP) to measure the mobility of DsRed Express, a tetrameric protein with a total molecular weight of 100 kD, the spine-residence time was 0.45 ± 0.03 s, still about 5-fold faster than that of PKA-C.

N-terminal myristoylation contributes to the low mobility of PKA-C

The spine-residence time of PKA-C-paGFP is comparable to HRas, KRas and the protein kinase C (PKC) substrate MARCKS protein (Figure 2C) (see also (Harvey et al., 2008)), which peripherally associates with the membrane via lipid modifications. In most parts of the brain, the majority of PKA-C isoforms are co-translationally myristoylated at their N-termini (Gangal et al., 1999; Guthrie et al., 1997; Johnson et al., 2001; Shoji et al., 1983), although this lipid modification is generally thought to fold into a hydrophobic pocket of

PKA-C to enhance its stability (Bastidas et al., 2013; Clegg et al., 1989; Yonemoto et al., 1993; Zheng et al., 1993).

We asked whether myristoylation is responsible for the low mobility of PKA-C. The myristoylation site was mutated by changing glycine at position two to alanine (G2A). This mutation did not affect the interaction between PKA-C and the PKA-R/AKAP complex (Figure S3) or the catalytic efficiency of the enzyme (for the latter, see (Clegg et al., 1989)). The resulting mutant, nmPKA-C-paGFP, moved significantly faster than wildtype (τ = 0.73 ± 0.03 s for NE stimulation, Figure 2A – 2C; and τ = 0.83 ± 0.03 for forskolin and IBMX stimulation, Figure 2D; for both, $p < 0.001$ c.f. wildtype), albeit still slower than paGFP. A testis-specific, naturally-occurring alternative splice isoform of PKA-C, which lacks the myristoylation site (named altPKA-C) (Desseyn et al., 2000; San Agustin et al., 1998), also moved more rapidly than the myristoylated neuronal isoform (τ = 0.85 ± 0.04 s, $p < 0.001$) (Figure 2D). Furthermore, addition of the PKA-C myristoylation sequence (N-terminal 47 residues) to paGFP appeared sufficient to slow down the diffusion of paGFP by more than 7-fold (construct named PKA-Cn-paGFP, τ = 1.96 ± 0.14 s, $p < 0.001$ c.f. paGFP) in a myristoylation-dependent manner (τ = 0.36 ± 0.02 s for nmPKA-Cn-paGFP, $p < 0.001$ c.f. PKA-Cn-paGFP) (Figure 2D). Therefore, the low mobility is intrinsic to PKA-C and is unlikely due to the residual interaction of liberated PKA-C with PKA-R. The simplest explanation of these results would be that myristoylation associates PKA-C with the membrane.

PKA-C becomes associated with the membrane upon activation

To address whether liberated PKA-C indeed associates with the membrane, we imaged PKA-C movement before and after activation in CA1 neurons. We expressed PKA-C-EGFP and PKA-RIIβ along with a cytosolic marker (DsRed Express or mCherry) and measured the intensity profile of PKA-C-EGFP along a line transecting thick (>=1.5 μm) primary apical dendrites and compared it to that of the cytosolic marker (Figure 3A). PKA-C-EGFP distributed similarly to the cytosolic marker at rest. However, upon stimulation of PKA activity, an increase in peripheral PKA-C-EGFP fluorescence and a decrease at the center of the dendrite was observed (Figure 3A), suggesting a translocation of PKA-C to the plasma membrane. To quantify this phenomenon, we computed a membrane enrichment index (MEI):

$$MEI = \frac{[F_{green}/F_{red}]_{peripheral}}{[F_{green}/F_{red}]_{center}}$$

where F is the fluorescence intensity. The peripheral fluorescence intensities were measured at a location approximating the edge of the dendrite (Figure 3A, lower panels), as determined by the location where the red fluorescence was 30% of the peak fluorescence (Figure S4). A value of MEI greater than 1 indicates membrane enrichment, whereas a value less than 1 indicates membrane exclusion. For wildtype PKA-C at rest, the MEI was slightly below one (MEI = 0.89 ± 0.02, $p<0.01$, c.f. 1), similar to that of PKA-RIIβ (MEI = 0.88 ± 0.02, $p = 0.67$, c.f. PKA-C) (Figure 3B), indicating a cytosolic localization of the protein. Stimulation of PKA with norepinephrine resulted in an increase in MEI (0.95 ± 0.03, p=0.01

c.f. baseline). MEI further increased to well above 1 with forskolin and IBMX (1.41 ± 0.03, p<0.001). The distribution of PKA-RIIβ did not change significantly upon stimulations (Figure 3B). Thus, only liberated PKA-C translocated to associate with the membrane.

The MEI value of PKA-C upon stimulation appears to be moderate. This is likely because only a fraction of PKA-C was liberated and the remaining PKA-C was still in the cytosol (Figure 1C and S1). Liberated PKA-C may also have affinity to intracellular membranes. To confirm that liberated PKA-C associates with the membrane, we co-expressed PKA-C-EGFP, PKA-RIIβ and mCherry labeled MARCKS, which is a known membrane substrate of PKC (Sundaram et al., 2004), in CA1 neurons (see Figure S5A for experimental design). Membrane association of PKA-C-EGFP would result in an increase in FRET between EGFP and mCherry and a corresponding decrease in EGFP lifetime. The fluorescence lifetime of EGFP decreased upon stimulation by forskolin and IBMX (Figure 3C and 3D; see also Figure S5B and S5C and their legends regarding the cluster noise seen in Figure 3C). Such a decrease in lifetime was not observed when EGFP was expressed alone, or when cytosolic mCherry was used in place of MARCKS-mCherry. This experiment further suggests that at least a portion of PKA-C associates with the membrane upon activation.

Does the association of PKA-C with the membrane require myristoylation? The translocation of PKA-C to the plasma membrane was greatly diminished, but not completely eliminated, when the myristoylation modification was abolished by the G2A mutation (before activation, MEI = 0.96 ± 0.05, p = 0.2, c.f. wildtype; and after forskolin/IBMX activation, 1.10 ± 0.02, p < 0.001, c.f. wildtype, and p = 0.02, c.f. 1) or by the naturally-occurring alternative splicing variant (before activation, MEI = 0.93 ± 0.03, p = 0.39, c.f. wildtype; and after activation, 1.10 ± 0.02, p < 0.001, c.f. wildtype, and p < 0.01, c.f. 1) (Figure 3B). Together, these results suggest that, under basal conditions, PKA-C is distributed in the cytosol of resting dendrites, where it is bound to the PKA-R/AKAP complex. Upon elevation of cAMP and release from PKA-R, the freed PKA-C translocates to the membrane, in large part requiring its N-terminal myristoylation.

Membrane association of PKA-C does not require AKAP anchoring

We asked whether the anchoring of PKA-R to AKAP affects the affinity of PKA-C with the membrane. When PKA-C was co-expressed with PKA-RIIβ-Δ 2–5, which no longer binds AKAPs (Figure S3) (Hausken et al., 1994; Zhong et al., 2009), the MEI of activated PKA-C reached the same level as when wildtype PKA-RIIβ was used (MEI = 1.38 ± 0.05 for PKA-RIIβ-Δ2–5 after forskolin/IBMX activation, p = 0.6, c.f. wildtype PKA-RIIβ; Figure 3B), indicating that the membrane affinity of PKA-C does not require AKAP binding. A further prediction is that, when PKA-C is co-expressed with PKA-RIIβ-Δ2–5, which no longer binds to AKAPs, its mobility should be high before activation because the PKA holoenzyme is no longer anchored. Upon activation, the mobility of PKA-C would decline as it becomes associated with the membrane. This was indeed the case (Figure 4). When PKA-RIIβ-Δ2–5 was co-expressed, the baseline spine-residence time of PKA-C-paGFP was 1.57 ± 0.07 s, which was slower than paGFP possibly due to the *ca.* 8-fold larger size (~220 kD for the holoenzyme with the paGFP tag) and the nonglobular shape of PKA-R (Smith et al., 2013). This construct however still moved faster than activated PKA-C with the co-expression of

wildtype PKA-RIIβ ($p < 0.001$). Upon stimulation by forskolin and IBMX, the spine-residence time increased to 2.59 ± 0.13 s ($p < 0.001$, c.f. before activation) (Figure 4). As a control, the spine-residence time of PKA-RIIβ-Δ2–5-paGFP did not change before and after stimulation (before stimulation, 1.60 ± 0.09 s; and after stimulation, 1.55 ± 0.10 s; $p = 0.68$; Figure 4B). Together with the evidence that the N-terminal 47 residues are sufficient for low PKA-C mobility (Figure 2D) and for enrichment on the membrane (Figure 3B), the membrane affinity is likely an intrinsic property of PKA-C and does not require AKAP anchoring. It should be noted, however, that AKAPs may still play a role in which membrane PKA-C become associated with.

Endogenous PKA activity is enriched on the membrane

The above experiments involved overexpression of PKA subunits. Does endogenous PKA-C also associate with the membrane? MEIs at the non-overexpression condition were estimated via extrapolation from the correlation between MEI values and the corresponding PKA-C-EGFP expression levels (Figure S6). The resulting values (MEI = 0.92 before activation and 1.42 after forskolin and IBMX activation) indicate that endogenous PKA-C also undergoes stimulation-dependent translocation to the membrane. Furthermore, this model predicts that endogenous PKA kinase activity should be higher on the membrane. To test this prediction, we used 2pFLIM to image the A-kinase activity reporter (AKAR) (Zhang et al., 2001). We optimized a recent version of AKAR (AKAR4) (Depry et al., 2011) for 2pFLIM by changing the donor and acceptor fluorophore pair to monomeric EGFP and sREACh. This new sensor was named AKAR5. Two additional variants were also generated: 1) a membrane-associated version (named m-AKAR5) by tagging AKAR5 with the C-terminal 15 amino-acid residues of KRas (Hancock et al., 1989), and 2) a cytosol-only version (named cyt-AKAR5) by linking AKAR5 to a nucleus-export sequence (NES) (Fukuda et al., 1996). Independently, similar improvements on AKAR have been recently reported (Chen et al., 2014).

We compared the responses of cyt-AKAR5 and m-AKAR5 to PKA stimulations under identical conditions in HEK 293 cells. To do so, m-AKAR5 was co-transfected with the nuclear marker mCherry-histone2b (red). Such transfected cells were then co-plated with other cells transfected with only cyt-AKAR5. As such, within the same field of view, cells that had red nuclei expressed m-AKAR5, while the other cells expressed cyt-AKAR5 (Figure 5A). At rest, m-AKAR5 exhibited an EGFP lifetime significantly lower than did cyt-AKAR5 (Figure 5A, represented by the warmer color in the 2pFLIM image at rest), presumably reflecting a basal cAMP concentration resulting in a low level of PKA activity already enriched on the membrane. Importantly, a mild stimulation with 0.1-μM norepinephrine strongly activated m-AKAR5 to 88± 6% of the maximal response induced by forskolin and IBMX (Figure 5B). Under the same conditions, cyt-AKAR5 was moderately activated (41 ± 7%, $p<0.001$). This difference between cyt-AKAR5 and m-AKAR5 was not due to higher phosphatase activity in the cytosol because, upon application of the broad spectrum phosphatase inhibitor okadaic acid (Bialojan and Takai, 1988; Reinhart et al., 1991), only m-AKAR5 but not cyt-AKAR5 responded with a higher level of phosphorylation (Figure 5C). Therefore, m-AKAR5 is more readily phosphorylated, suggesting that endogenous PKA kinase activity is enriched on the membrane.

Is endogenous PKA activity also enriched on the membrane in neurons? A variant of AKAR5 (named AKAR5′ in which a circularly-permuted version of sREACh was used to mimic the circularly-permuted Venus used in AKAR4 (Depry et al., 2011)) and its membrane-associated version (m-AKAR5′) were expressed, respectively, in CA1 neurons in cultured slices. Mild stimulation of the PKA pathway via norepinephrine (0.3 μM) led to nearly saturating responses on m-AKAR5′ but only moderately activated the cytosolic AKAR5′ (85 ± 5% of maximal response for m-AKAR5′, and 50 ± 8% for AKAR5′; $p < 0.01$) (Figure 5D). This result indicates that endogenous PKA kinase activity is also enriched on the membrane in neurons.

PKA preferentially phosphorylates substrates residing on the membrane in a myristoylation dependent manner

If PKA activity is enriched on the membrane, a substrate on the membrane would be preferentially phosphorylated compared to the same substrate in the cytosol. We tested this prediction by using the AMPA receptor subunit GluA1, which can be phosphorylated at its C-terminal tail at serine 845 by PKA (Colledge et al., 2000; Lee et al., 2000). EGFP-tagged GluA1 or its cytosolic C-tail (GluA1c) was expressed (Figure 6A) and their phosphorylation levels were quantified by normalizing the western-blot signal from a phospho-S845 specific antibody to that from a general GluA1 C-terminal antibody. In both HEK 293 cells (Figure 6B and 6C) and in cortical primary neuronal cultures (Figure 6D and 6E), EGFP-GluA1 was robustly phosphorylated when cells were stimulated by norepinephrine or forskolin/IBMX. This phosphorylation was blocked by the PKA antagonist H89. However, under the same conditions, the phosphorylation of EGFP-GluA1c was nearly undetectable. The phosphorylation of EGFP-GluA1c was rescued by tethering it to the membrane via fusion to an irrelevant, single-transmembrane protein CD4 (construct named CD4-EGFP-GluA1c, Figure 6A, 6B and 6C). Thus, this substrate is more effectively phosphorylated by endogenous PKA when it is on the membrane.

The preferential phosphorylation of membrane substrates also appeared to be intrinsic to PKA-C and independent of AKAPs. We co-expressed EGFP-GluA1 and EGFP-GluA1c in HEK 293 cells and treated the cells with norepinephrine or forskolin/IBMX in the presence of a membrane-permeant peptide St-Ht31 (20 μM), which disrupts AKAP binding to PKA (Carr et al., 1992). This treatment did not decrease the PKA phosphorylation of EGFP-GluA1 nor increase the phosphorylation of EGFP-GluA1c (Figure 6F and 6G). The St-Ht31 treatment appeared to be effective as it significantly reduced the binding of PKA-C and PKA-RIIβ to EGFP-AKAP5 in a co-IP assay (Figure 6H and 6I).

Does the preferential phosphorylation of membrane substrates by PKA involve myristoylation? To test this possibility, we expressed PKA-C-EGFP or nmPKA-C-EGFP, respectively, along with PKA-RIIβ, EGFP-GluA1, and EGFP-GluA1c in the same cells, and compare the phosphorylation levels on the membrane and in the cytosol by using a membrane-phosphorylation preference index:

$$MPPI = \frac{[pS845/total]_{GluA1}}{[pS845/total]_{GluA1c}}$$

Higher MPPIs reflect a higher preference to phosphorylate a membrane substrate over the same substrate in the cytosol. High MPPIs were measured if wildtype PKA-C-EGFP was expressed ($MPPI_{NE,\ PKA\text{-}C} = 9.9 \pm 1.7$, and $MPPI_{F/I,\ PKA\text{-}C} = 7.1 \pm 1.3$; Figure 6J, 6K and 6L). However, MPPIs were significantly reduced when nmPKA-C-EGFP was expressed instead, although EGFP-GluA1 was still preferentially phosphorylated ($MPPI_{NE,\ nmPKA\text{-}C} = 2.9 \pm 1.0$, and $MPPI_{F/I,\ nmPKA\text{-}C} = 3.0 \pm 0.4$; for both, $p < 0.001$, c.f. wildtype; Figure 6L). Endogenous myristoylated PKA activity and a residual membrane affinity of nmPKA-C (Figure 3B) may account for this remaining preference. Together, these results indicate a critical role of the myristoylation in PKA-C's ability to preferentially phosphorylate membrane substrates.

PKA-C myristoylation is important for PKA regulation of synaptic function and plasticity

Is PKA-C myristoylation important for neuronal function? We addressed this question by performing two independent experiments. First, PKA is known to play important roles in the regulation of synaptic plasticity (Ehrlich and Malinow, 2004; Thomas et al., 1996; Tzounopoulos et al., 1998; Weisskopf et al., 1994; Yasuda et al., 2003). We overexpressed wildtype or non-myristoylated PKA-C-EGFP with PKA-RIIβ in CA1 neurons of cultured hippocampal slices, and triggered single-spine structural long-term potentiation (LTP) using two-photon glutamate uncaging at individual spines of oblique apical dendrites (Matsuzaki et al., 2004). When wildtype PKA-C was expressed, glutamate uncaging triggered a long-lasting potentiation of the volume of activated dendritic spines but not adjacent control spines (potentiation = 73 ± 18% for stimulated spines, and −7 ± 8% for control spines, $n = 9$, $p < 0.001$) (Figure 7A, 7B and 7C). The amplitude of potentiation was indistinguishable from control, GFP-transfected neurons (potentiation = 82 ± 28%, $n = 5$, $p = 0.8$, c.f. wildtype PKA-C) (Figure 7C). However, this potentiation was nearly abolished if nmPKA-C-EGFP was expressed (potentiation = 14 ± 9% for activated spines, $n = 10$, $p < 0.01$ c.f. wildtype PKA-C). This dominant effect of nmPKA-C may be due to undesired higher PKA activity in the cytosol, although other explanations are also possible. Regardless of the mechanism, the fact that neurons can tolerate the expression of wildtype but not non-myristoylated PKA-C indicates the functional importance of the myristoylation.

Second, to examine the role of myristoylation of endogenous PKA in regulating synaptic transmission, we developed a shRNA construct (sh-PKA-C) to selectively knock down PKA-C alpha subunit (Figure S7A). PKA facilitates the synaptic insertion of AMPA receptors (Ehrlich and Malinow, 2004). Consistently, neurons expressing sh-PKA-C exhibited significantly lower AMPA receptor currents compared to paired, adjacent untransfected neurons (Figure 7D1, S7B, S7C and S7D). A small decrease in the amplitude, but not the frequency, of miniature excitatory postsynaptic currents (mEPSC) was also observed (Figure S7E, S7F and S7G). Although PKA is also known to regulate NMDA receptors (Murphy et al., 2014; Scott et al., 2003; Tingley et al., 1997), the effect of PKA knockdown on NMDA receptor currents was small and not statistically significant (Figure 7E1, $p = 0.16$, $n = 15$). As a result, the AMPA/NMDA current ratio was reduced (Figure S7D). The paired pulse ratio (PPR), a presynaptic function indicator, was unaltered (Figure S7H and S7I). The reduced AMPA current and AMAP/NMDA current ratio were rescued by co-expressing an shRNA-resistant PKA-C-EGFP construct (r.PKA-C) (Figure S7A, 7D2 and

S7D), but not if the myristoylation was abolished in the rescuing construct (r.nmPKA-C) (Figure 7D3 and S7D). This result indicates that the myristoylation is essential for normal PKA regulation of synaptic function. Together, PKA myristoylation appears to be important for normal PKA regulation of synaptic function and structural plasticity.

DISCUSSION

The activation-dependent translocation of PKA-C to the membrane revises the prevalent model of PKA action in which liberated PKA-C is thought to remain in the cytosol. Although co-IP was recently used to suggest that most PKA-C remains bound to PKA-R in HEK cells following stimulation of β-adrenergic receptors (Smith et al., 2013), this experiment cannot rule out that a fraction of PKA-C molecules is liberated. In the brain, the synaptic release of neuromodulators may result in high local concentrations (>= 100 μM) of norepinephrine and dopamine (Courtney and Ford, 2014; Ford et al., 2009). Compared to HEK cells, neurons may also express higher levels of components of the PKA activating pathway, such as adrenergic receptors, G proteins and adenylyl cyclases, to promote PKA activation and liberation (c.f. Figure 1C and Figure S1). The present results indicate that at least a fraction (> 10%) of PKA-C leaves the PKA-R/AKAP complex in hippocampal CA1 neurons with norepinephrine stimulation at a concentration well below the maximum concentration a neuron might experience (Figure 1). Once PKA-C leaves PKA-R, its activity increases by over 50-fold (Beavo et al., 1974a; Miyamoto et al., 1969; Reimann et al., 1971). A 10% release of PKA-C may therefore result in an over 5-fold increase in kinase activity.

This revised model explains why activated PKA-C becomes enriched in dendritic spines (Figure 1E) (Zhong et al., 2009): spines have a much higher membrane to cytosol ratio compared to dendritic shafts. This model also works in concert with current understanding of how PKA achieves its specificity. AKAPs establish the initial spatial localization and specificity of PKA. However, it has been less clear how such specificity can be sustained after PKA-C is liberated. Membrane association of liberated PKA-C may enhance PKA specificity in multiple ways. First, the membrane becomes a distinct compartment for PKA signaling. Several studies have suggested that PKA kinase activity is higher at the plasma membrane (Castro et al., 2010; Terrin et al., 2006). Although these results have been attributed to a higher local cAMP concentration near the membrane, our finding suggests that the intrinsic membrane affinity of liberated PKA-C may also contribute. Second, membrane-associated PKA-C moves more slowly than a typical cytosolic protein (Figure 2). This is presumably due to the high viscosity of the membrane when PKA-C diffuses along the membrane, although it cannot be ruled out that PKA-C diffuses within the cytosol, and membrane association limits the availability of PKA-C for diffusion. Regardless of the precise mechanism, a low mobility would promote signaling compartmentalization. Third, although PKA-C's membrane affinity does not require AKAPs, AKAP anchoring of holo-PKA may influence where liberated PKA-C is inserted. Once PKA-C is inserted into the membrane, the likelihood of PKA-C moving from one membrane structure to the cytosol or to a discontinuous membrane structure is reduced, thereby sustaining AKAP-mediated PKA specificity. Finally, while the membrane association of PKA-C may not be the only mechanism for maintaining PKA specificity, it exemplifies the existence of mechanisms for

phosphorylation specificity downstream of AKAPs and their potentially important roles in cellular function.

The membrane association of liberated PKA-C is mediated largely by the N-terminal myristoylation. In the crystal structure, this myristoyl group was found to fold into a hydrophobic pocket within PKA-C (Zheng et al., 1993). Additional studies suggested that a function of the myristoylation was to enhance protein stability (Herberg et al., 1997; Yonemoto et al., 1993). These findings, together with the fact that PKA-C appears to be highly soluble (Johnson et al., 2001), have led to the prevalent view that PKA-C is a cytosolic protein. Nevertheless, it has also been suggested that the myristoyl group can be exposed when PKA-C binds to the type II PKA-R or when it is phosphorylated at the serine residue at position 11 (S11) (Gaffarogullari et al., 2011; Gangal et al., 1999; Zhang et al., 2015), and that, when exposed, the myristoyl group can be inserted into reconstituted lipid bilayers (Gaffarogullari et al., 2011; Struppe et al., 1998; Zhang et al., 2015). However, it remained obscure whether and under what circumstances this modification associates PKA with the membrane *in vivo*. For example, it was suggested that the type II PKA holoenzyme can associate with reconstituted lipid bilayers (Zhang et al., 2015). Our study instead indicates that liberated PKA-C, but not holo-PKA, associates with the membrane in living neurons. An implication is that the myristoyl group of PKA-C can be exposed in the absence of PKA-R. In addition, S11 appears to play a relatively minor role in the membrane targeting: abolishing this phosphorylation site (S11A) decreased the spine residence time only moderately (30% faster, Figure 2D), and the phosphorylation-mimicking mutant S11D moved even slightly faster than the S11A mutant (Figure 2D).

The membrane affinity of PKA-C is likely at a mid-range for reversible association. The N-terminal 14 residues of PKA-C, when swapped into the Src protein, provide only a low level of membrane association (Silverman and Resh, 1992). This is consistent with the prevalent view that myristoylation usually requires a second lipid affinity motif for membrane targeting. Such a motif, if it exists, may also account for the residual membrane affinity in nmPKA-C (Figure 3B). The N-terminal 47 residues of PKA-C are sufficient to slow protein diffusion (Figure 2D) and to associate with the membrane (Figure 3B), suggesting that the second lipid affinity motif is likely present within this PKA-C fragment. Whether or not the second motif exists, neuronal dendrites are rich in membranes, which may compensate for a finite membrane affinity. A finite affinity to the membrane may also be important in the termination of PKA signaling as liberated PKA-C must eventually return to PKA-R within the cytosol.

Our results suggest that the majority of liberated PKA-C is located on the membrane in dendrites as the spine-residence time decay curve was well fit by a single exponential (Figure 1B), suggesting that there is not a significant fraction of fast diffusing PKA-C. At the same time, it cannot be ruled out that a small fraction of liberated PKA-C remains in the cytosol. Our data also suggests that the plasma membrane is one of the primary locations for activated PKA-C (e.g., Figure 3A and 3B). However, PKA-C likely also has affinity for intracellular membranes, such as the ER. On the other hand, although direct membrane association is the simplest explanation of our data, we cannot rule out the possibility that

PKA-C in fact binds to an abundant, membrane-distributed protein in a myristoylation dependent manner, albeit such a protein has not been previously documented.

How does PKA-C regulate substrates in the cytosol? There may be several mechanisms. First, as discussed above, the myristoyl group of PKA-C is likely to have a finite affinity to the membrane, and PKA-C may cycle on and off between the membrane and the cytosol. Second, cytosolic proteins may travel to the membrane transiently, get phosphorylated and then move back to the cytosol. Third, not all PKA-C leaves PKA-R even when strongly stimulated, but the pool of unreleased PKA-C may exhibit a certain level of activity (Smith et al., 2013). It should also be noted that in certain part of the brain and at a low level throughout the brain, alternative splicing variants of the PKA-C beta subunit lacking the myrstoylation site are expressed in addition to myristoylated PKA-C (Guthrie et al., 1997). Although the precise abundance and function of these non-myristoylated PKA-C variants are not known, they may contribute to the phosphorylation of cytosolic substrates. In any case, cytosolic AKAR5 can still be phosphorylated by PKA, albeit with less sensitivity than membrane-residing AKAR5. On the other hand, why does PKA phosphorylate cytosolic AKAR5 with little phosphorylation of GluA1c (c.f. Figure 5B and 6B)? Different substrates may have different sensitivities to PKA phosphorylation (e.g., see (Beavo et al., 1974b)). In AKAR5, a phospho-residue binding domain may protect the site from phosphatase activities, so that moderate PKA activity may integrate over time to result in significant phosphorylation of the sensor.

What is the distribution of PKA-C before it is liberated? In its inactivated state, PKA-C binds to PKA-R, which in turn binds to AKAPs. In neuronal dendrites, the most abundant AKAP is the microtubule-binding protein MAP2 (Zhong et al., 2009). Therefore, the majority of PKA likely resides in the cytosol and is anchored to microtubules (Figure 2A). This is consistent with that fact that the MEI for wildtype PKA at rest is smaller than unity in neuronal dendrites (Figure 3). Overall, our results suggest a modified view of how the PKA catalytic subunit functions in neurons.

EXPERIMENTAL PROCEDURES

Plasmid constructs

Constructs were made using standard mutagenesis and subcloning methods. See SUPPLEMENTAL EXPERIMENTAL PROCEDURES for detailed descriptions of each construct. All previously unpublished constructs and their sequences will be deposited to Addgene upon acceptance of the manuscript.

Organotypic hippocampal slice cultures and transfections

Rat hippocampal slice cultures were prepared from P6 – P7 pups as previously described (Stoppini et al., 1991; Zhong et al., 2009). Animal handling and experimental protocols were performed in accordance with the recommendations in the Guide for the Care and Use of Laboratory Animals of the National Institutes of Health, and were approved by the Institutional Animal Care and Use Committee (IACUC) of the Oregon Health & Science University (#IS00002792). cDNA constructs were transfected after 2 – 3 weeks *in vitro* via

biolistic gene transfer using the Helios gene gun and 1.6 μm gold beads, or with single cell electroporation (electroporation was used for Figure 7D – 7G and Figure S7) (Otmakhov and Lisman, 2012).

Cell cultures, transfection, and biochemistry

HEK 293 cells and primary cultures of cortical neurons (Xu et al., 2010) were prepared following standard protocols and transfected using Lipofectamine 2000 (Invitrogen) and electroporation, respectively. Co-IP experiments were performed following standard procedures using the appropriate antibody with magnetic protein G beads (Life Technologies Novex 10007D). Western blots were carried out using either 7% fixed or 7 – 10% gradient polyacrylamide gels and detected with a LI-COR Odyssey scanner (Figure 6B, 6C, 6J, 6K, and 6L) or with chemiluminescence. See SUPPLEMENTAL EXPERIMENTAL PROCEDURES for details.

Imaging, uncaging and electrophysiology

Imaging including 2pFLIM were carried out as previously described (Harvey et al., 2008; Yasuda et al., 2006; Zhong et al., 2009) using a custom built setup controlled by the ScanImage software (Pologruto et al., 2003).

Whole-cell voltage-clamp recordings were performed using a MultiClamp 700B amplifier (Molecular Devices) controlled with custom software written in MATLAB. Electrophysiological signals were filtered at 2 kHz and digitized at 20 kHz. Slices were perfused with artificial cerebrospinal fluid (ACSF) containing 4 mM Ca and 4 mM Mg. The internal solution contained (in mM) 132 Cs-gluconate, 10 HEPES, 10 Na-phosphocreatine, 4 MgCl2, 4 Na2-ATP, 0.4 Na-GTP, 3 Na-ascorbate, 3 QX314, 0.2 EGTA with an osmolarity of 295 mOsmol/kg. To reduce recurrent activities, cultured hippocampal slices were cut on both sides of CA1 and 4μM 2-chloroadenosine (Sigma) was present in all recording experiments. 10 μM GABAzine (SR 95531, Tocris) was also included to suppress GABA currents.

Further details can be found at SUPPLEMENTAL EXPERIMENTAL PROCEDURES.

Data analysis, presentation, and statistics

Image analysis was done using custom software written in MATLAB. See SUPPLEMENTAL EXPERIMENTAL PROCEDURES for details. Averaged data are presented as mean ± SEM unless noted otherwise. n indicates the number of experiments. p values were obtained from ANOVA tests, unless noted otherwise. In all figures, *: $p <= 0.01$, and **: $p <= 0.001$.

Supplementary Material

Refer to Web version on PubMed Central for supplementary material.

Acknowledgments

We thank Drs. John Scott, Wolfhard Almers, Craig Jahr, John Adelman, Paul Brehm, John Williams, Bart Jongbloets, Tianyi Mao and King-Wai Yau, and Mr. Josh Melander for helpful discussions and comments. We thank Dr. Jin Zhang for providing the AKAR4 cDNA, Dr. Bo Li for the EGFP-GluA1 cDNA, Dr. Peter Barr-Gillespie for the mouse monoclonal anti-GFP antibody, Dr. Ryohei Yasuda for 2pFLIM acquisition software, Dr. Michael Cohen for the EF1Ub-300 EGFP plasmid, Dr. Nikolai Otmakhov and John Lisman for the single-cell electroporation technique, and Dr. Jun Xia for helps in primary neuronal culture. This work was supported by a NIH NRSA F31NS079083 (S.T.), a NIH New Innovator Award DP2OD008425 (H.Z.), a Medical Research Foundation grant (H.Z.), a National Alliance for Research on Schizophrenia and Depression Young Investigator Award (H.Z.) and a NIH R01 grant R01DK090309 (P.S.).

References

Bastidas AC, Pierce LC, Walker RC, Johnson DA, Taylor SS. Influence of N-myristylation and ligand binding on the flexibility of the catalytic subunit of protein kinase A. Biochemistry. 2013; 52:6368–6379. [PubMed: 24003983]

Beavo JA, Bechtel PJ, Krebs EG. Activation of protein kinase by physiological concentrations of cyclic AMP. Proc Natl Acad Sci U S A. 1974a; 71:3580–3583. [PubMed: 4372627]

Beavo JA, Bechtel PJ, Krebs EG. Preparation of homogeneous cyclic AMP-dependent protein kinase(s) and its subunits from rabbit skeletal muscle. Methods Enzymol. 1974b; 38:299–308. [PubMed: 4375763]

Bialojan C, Takai A. Inhibitory effect of a marine-sponge toxin, okadaic acid, on protein phosphatases. Specificity and kinetics. Biochem J. 1988; 256:283–290. [PubMed: 2851982]

Bloodgood BL, Sabatini BL. Neuronal activity regulates diffusion across the neck of dendritic spines. Science. 2005; 310:866–869. [PubMed: 16272125]

Brooker G. Oscillation of cyclic adenosine monophosphate concentration during the myocardial contraction cycle. Science. 1973; 182:933–934. [PubMed: 4355524]

Buxton IL, Brunton LL. Compartments of cyclic AMP and protein kinase in mammalian cardiomyocytes. J Biol Chem. 1983; 258:10233–10239. [PubMed: 6309796]

Carr DW, Stofko-Hahn RE, Fraser ID, Cone RD, Scott JD. Localization of the cAMP-dependent protein kinase to the postsynaptic densities by A-kinase anchoring proteins. Characterization of AKAP 79. J Biol Chem. 1992; 267:16816–16823. [PubMed: 1512224]

Castro LR, Gervasi N, Guiot E, Cavellini L, Nikolaev VO, Paupardin-Tritsch D, Vincent P. Type 4 phosphodiesterase plays different integrating roles in different cellular domains in pyramidal cortical neurons. J Neurosci. 2010; 30:6143–6151. [PubMed: 20427672]

Chen Y, Saulnier JL, Yellen G, Sabatini BL. A PKA activity sensor for quantitative analysis of endogenous GPCR signaling via 2-photon FRET-FLIM imaging. Front Pharmacol. 2014; 5:56. [PubMed: 24765076]

Clegg CH, Ran W, Uhler MD, McKnight GS. A mutation in the catalytic subunit of protein kinase A prevents myristylation but does not inhibit biological activity. J Biol Chem. 1989; 264:20140–20146. [PubMed: 2584209]

Colledge M, Dean RA, Scott GK, Langeberg LK, Huganir RL, Scott JD. Targeting of PKA to glutamate receptors through a MAGUK-AKAP complex. Neuron. 2000; 27:107–119. [PubMed: 10939335]

Courtney NA, Ford CP. The timing of dopamine- and noradrenaline-mediated transmission reflects underlying differences in the extent of spillover and pooling. J Neurosci. 2014; 34:7645–7656. [PubMed: 24872568]

Davare MA, Avdonin V, Hall DD, Peden EM, Burette A, Weinberg RJ, Horne MC, Hoshi T, Hell JW. A β_2 adrenergic receptor signaling complex assembled with the Ca^{2+} channel $Ca_V1.2$. Science. 2001; 293:98–101. [PubMed: 11441182]

Depry C, Allen MD, Zhang J. Visualization of PKA activity in plasma membrane microdomains. Mol Biosyst. 2011; 7:52–58. [PubMed: 20838685]

Desseyn JL, Burton KA, McKnight GS. Expression of a nonmyristylated variant of the catalytic subunit of protein kinase A during male germ-cell development. Proc Natl Acad Sci U S A. 2000; 97:6433–6438. [PubMed: 10841548]

Dunn TA, Wang CT, Colicos MA, Zaccolo M, DiPilato LM, Zhang J, Tsien RY, Feller MB. Imaging of cAMP levels and protein kinase A activity reveals that retinal waves drive oscillations in second-messenger cascades. J Neurosci. 2006; 26:12807–12815. [PubMed: 17151284]

Ehrlich I, Malinow R. Postsynaptic density 95 controls AMPA receptor incorporation during long-term potentiation and experience-driven synaptic plasticity. J Neurosci. 2004; 24:916–927. [PubMed: 14749436]

Flockhart DA, Corbin JD. Regulatory mechanisms in the control of protein kinases. CRC Crit Rev Biochem. 1982; 12:133–186. [PubMed: 7039969]

Ford CP, Phillips PE, Williams JT. The time course of dopamine transmission in the ventral tegmental area. J Neurosci. 2009; 29:13344–13352. [PubMed: 19846722]

Francis SH, Corbin JD. Structure and function of cyclic nucleotide-dependent protein kinases. Annu Rev Physiol. 1994; 56:237–272. [PubMed: 8010741]

Fukuda M, Gotoh I, Gotoh Y, Nishida E. Cytoplasmic localization of mitogen-activated protein kinase kinase directed by its NH2-terminal, leucine-rich short amino acid sequence, which acts as a nuclear export signal. J Biol Chem. 1996; 271:20024–20028. [PubMed: 8702720]

Gaffarogullari EC, Masterson LR, Metcalfe EE, Traaseth NJ, Balatri E, Musa MM, Mullen D, Distefano MD, Veglia G. A myristoyl/phosphoserine switch controls cAMP-dependent protein kinase association to membranes. J Mol Biol. 2011; 411:823–836. [PubMed: 21740913]

Gangal M, Clifford T, Deich J, Cheng X, Taylor SS, Johnson DA. Mobilization of the A-kinase N-myristate through an isoform-specific intermolecular switch. Proc Natl Acad Sci U S A. 1999; 96:12394–12399. [PubMed: 10535933]

Gorbunova YV, Spitzer NC. Dynamic interactions of cyclic AMP transients and spontaneous Ca(2+) spikes. Nature. 2002; 418:93–96. [PubMed: 12097913]

Gray NW, Weimer RM, Bureau I, Svoboda K. Rapid Redistribution of Synaptic PSD-95 in the Neocortex In Vivo. PLoS Biol. 2006; 4

Guthrie CR, Skalhegg BS, McKnight GS. Two novel brain-specific splice variants of the murine Cbeta gene of cAMP-dependent protein kinase. J Biol Chem. 1997; 272:29560–29565. [PubMed: 9368018]

Hancock JF, Magee AI, Childs JE, Marshall CJ. All ras proteins are polyisoprenylated but only some are palmitoylated. Cell. 1989; 57:1167–1177. [PubMed: 2661017]

Harvey CD, Yasuda R, Zhong H, Svoboda K. The spread of Ras activity triggered by activation of a single dendritic spine. Science. 2008; 321:136–140. [PubMed: 18556515]

Hausken ZE, Coghlan VM, Hastings CA, Reimann EM, Scott JD. Type II regulatory subunit (RII) of the cAMP-dependent protein kinase interaction with A-kinase anchor proteins requires isoleucines 3 and 5. J Biol Chem. 1994; 269:24245–24251. [PubMed: 7929081]

Herberg FW, Zimmermann B, McGlone M, Taylor SS. Importance of the A-helix of the catalytic subunit of cAMP-dependent protein kinase for stability and for orienting subdomains at the cleft interface. Protein Sci. 1997; 6:569–579. [PubMed: 9070439]

Johnson DA, Akamine P, Radzio-Andzelm E, Madhusudan M, Taylor SS. Dynamics of cAMP-dependent protein kinase. Chem Rev. 2001; 101:2243–2270. [PubMed: 11749372]

Johnson DA, Leathers VL, Martinez AM, Walsh DA, Fletcher WH. Fluorescence resonance energy transfer within a heterochromatic cAMP-dependent protein kinase holoenzyme under equilibrium conditions: new insights into the conformational changes that result in cAMP-dependent activation. Biochemistry. 1993; 32:6402–6410. [PubMed: 8390856]

Lee HK, Barbarosie M, Kameyama K, Bear MF, Huganir RL. Regulation of distinct AMPA receptor phosphorylation sites during bidirectional synaptic plasticity. Nature. 2000; 405:955–959. [PubMed: 10879537]

Lohmann SM, DeCamilli P, Einig I, Walter U. High-affinity binding of the regulatory subunit (RII) of cAMP-dependent protein kinase to microtubule-associated and other cellular proteins. Proc Natl Acad Sci U S A. 1984; 81:6723–6727. [PubMed: 6093118]

Lu Y, Allen M, Halt AR, Weisenhaus M, Dallapiazza RF, Hall DD, Usachev YM, McKnight GS, Hell JW. Age-dependent requirement of AKAP150-anchored PKA and GluR2-lacking AMPA receptors in LTP. Embo J. 2007; 26:4879–4890. [PubMed: 17972919]

Lu Y, Zhang M, Lim IA, Hall DD, Allen M, Medvedeva Y, McKnight GS, Usachev YM, Hell JW. AKAP150-anchored PKA activity is important for LTD during its induction phase. J Physiol. 2008; 586:4155–4164. [PubMed: 18617570]

Matsuzaki M, Honkura N, Ellis-Davies GC, Kasai H. Structural basis of long-term potentiation in single dendritic spines. Nature. 2004; 429:761–766. [PubMed: 15190253]

Miyamoto E, Kuo JF, Greengard P. Cyclic nucleotide-dependent protein kinases. 3. Purification and properties of adenosine 3′,5′-monophosphate-dependent protein kinase from bovine brain. J Biol Chem. 1969; 244:6395–6402. [PubMed: 4311198]

Murakoshi H, Lee SJ, Yasuda R. Highly sensitive and quantitative FRET-FLIM imaging in single dendritic spines using improved non-radiative YFP. Brain Cell Biol. 2008; 36:31–42. [PubMed: 18512154]

Murphy JA, Stein IS, Lau CG, Peixoto RT, Aman TK, Kaneko N, Aromolaran K, Saulnier JL, Popescu GK, Sabatini BL, et al. Phosphorylation of Ser1166 on GluN2B by PKA is critical to synaptic NMDA receptor function and Ca2+ signaling in spines. J Neurosci. 2014; 34:869–879. [PubMed: 24431445]

Ni Q, Ganesan A, Aye-Han NN, Gao X, Allen MD, Levchenko A, Zhang J. Signaling diversity of PKA achieved via a Ca2+-cAMP-PKA oscillatory circuit. Nat Chem Biol. 2010; 7:34–40. [PubMed: 21102470]

Otmakhov N, Lisman J. Measuring CaMKII concentration in dendritic spines. J Neurosci Methods. 2012; 203:106–114. [PubMed: 21985762]

Papadopoulos S, Jurgens KD, Gros G. Protein diffusion in living skeletal muscle fibers: dependence on protein size, fiber type, and contraction. Biophys J. 2000; 79:2084–2094. [PubMed: 11023912]

Parisiadou L, Yu J, Sgobio C, Xie C, Liu G, Sun L, Gu XL, Lin X, Crowley NA, Lovinger DM, Cai H. LRRK2 regulates synaptogenesis and dopamine receptor activation through modulation of PKA activity. Nat Neurosci. 2014; 17:367–376. [PubMed: 24464040]

Patterson GH, Lippincott-Schwartz J. A photoactivatable GFP for selective photolabeling of proteins and cells. Science. 2002; 297:1873–1877. [PubMed: 12228718]

Pologruto TA, Sabatini BL, Svoboda K. ScanImage: Flexible software for operating laser-scanning microscopes. BioMedical Engineering OnLine. 2003; 2:13. [PubMed: 12801419]

Reimann EM, Walsh DA, Krebs EG. Purification and properties of rabbit skeletal muscle adenosine 3′, 5′-monophosphate-dependent protein kinases. J Biol Chem. 1971; 246:1986–1995. [PubMed: 4324558]

Reinhart PH, Chung S, Martin BL, Brautigan DL, Levitan IB. Modulation of calcium-activated potassium channels from rat brain by protein kinase A and phosphatase 2A. J Neurosci. 1991; 11:1627–1635. [PubMed: 1646298]

San Agustin JT, Leszyk JD, Nuwaysir LM, Witman GB. The catalytic subunit of the cAMP-dependent protein kinase of ovine sperm flagella has a unique amino-terminal sequence. J Biol Chem. 1998; 273:24874–24883. [PubMed: 9733793]

Scott DB, Blanpied TA, Ehlers MD. Coordinated PKA and PKC phosphorylation suppresses RXR-mediated ER retention and regulates the surface delivery of NMDA receptors. Neuropharmacology. 2003; 45:755–767. [PubMed: 14529714]

Scott JD, Pawson T. Cell signaling in space and time: where proteins come together and when they're apart. Science. 2009; 326:1220–1224. [PubMed: 19965465]

Shoji S, Ericsson LH, Walsh KA, Fischer EH, Titani K. Amino acid sequence of the catalytic subunit of bovine type II adenosine cyclic 3′,5′-phosphate dependent protein kinase. Biochemistry. 1983; 22:3702–3709. [PubMed: 6311252]

Silverman L, Resh MD. Lysine residues form an integral component of a novel NH2-terminal membrane targeting motif for myristylated pp60v-src. J Cell Biol. 1992; 119:415–425. [PubMed: 1400583]

Smith FD, Reichow SL, Esseltine JL, Shi D, Langeberg LK, Scott JD, Gonen T. Intrinsic disorder within an AKAP-protein kinase A complex guides local substrate phosphorylation. Elife. 2013; 2:e01319. [PubMed: 24192038]

Stoppini L, Buchs PA, Muller DA. A simple method for organotypic cultures of nervous tissue. J Neurosci Methods. 1991; 37:173–182. [PubMed: 1715499]

Struppe J, Komives EA, Taylor SS, Vold RR. 2H NMR studies of a myristoylated peptide in neutral and acidic phospholipid bicelles. Biochemistry. 1998; 37:15523–15527. [PubMed: 9799515]

Sundaram M, Cook HW, Byers DM. The MARCKS family of phospholipid binding proteins: regulation of phospholipase D and other cellular components. Biochem Cell Biol. 2004; 82:191–200. [PubMed: 15052337]

Swaminathan R, Hoang CP, Verkman AS. Photobleaching recovery and anisotropy decay of green fluorescent protein GFP-S65T in solution and cells: cytoplasmic viscosity probed by green fluorescent protein translational and rotational diffusion. Biophys J. 1997; 72:1900–1907. [PubMed: 9083693]

Terrin A, Di Benedetto G, Pertegato V, Cheung YF, Baillie G, Lynch MJ, Elvassore N, Prinz A, Herberg FW, Houslay MD, Zaccolo M. PGE(1) stimulation of HEK293 cells generates multiple contiguous domains with different [cAMP]: role of compartmentalized phosphodiesterases. J Cell Biol. 2006; 175:441–451. [PubMed: 17088426]

Thomas MJ, Moody TD, Makhinson M, O'Dell TJ. Activity-dependent beta-adrenergic modulation of low frequency stimulation induced LTP in the hippocampal CA1 region. Neuron. 1996; 17:475–482. [PubMed: 8816710]

Tingley WG, Ehlers MD, Kameyama K, Doherty C, Ptak JB, Riley CT, Huganir RL. Characterization of protein kinase A and protein kinase C phosphorylation of the N-methyl-D-aspartate receptor NR1 subunit using phosphorylation site-specific antibodies. J Biol Chem. 1997; 272:5157–5166. [PubMed: 9030583]

Turnham RE, Scott JD. Protein kinase A catalytic subunit isoform PRKACA; History, function and physiology. Gene. 2016; 577:101–108. [PubMed: 26687711]

Tzounopoulos T, Janz R, Sudhof TC, Nicoll RA, Malenka RC. A role for cAMP in long-term depression at hippocampal mossy fiber synapses. Neuron. 1998; 21:837–845. [PubMed: 9808469]

Weisskopf MG, Castillo PE, Zalutsky RA, Nicoll RA. Mediation of hippocampal mossy fiber long-term potentiation by cyclic AMP. Science. 1994; 265:1878–1882. [PubMed: 7916482]

Wong W, Scott JD. AKAP signalling complexes: focal points in space and time. Nat Rev Mol Cell Biol. 2004; 5:959–970. [PubMed: 15573134]

Xu J, Xiao N, Xia J. Thrombospondin 1 accelerates synaptogenesis in hippocampal neurons through neuroligin 1. Nat Neurosci. 2010; 13:22–24. [PubMed: 19915562]

Yang S, Fletcher WH, Johnson DA. Regulation of cAMP-dependent protein kinase: enzyme activation without dissociation. Biochemistry. 1995; 34:6267–6271. [PubMed: 7756252]

Yasuda H, Barth AL, Stellwagen D, Malenka RC. A developmental switch in the signaling cascades for LTP induction. Nat Neurosci. 2003; 6:15–16. [PubMed: 12469130]

Yasuda R, Harvey CD, Zhong H, Sobczyk A, van Aelst L, Svoboda K. Supersensitive Ras activation in dendrites and spines revealed by two-photon fluorescence lifetime imaging. Nat Neurosci. 2006; 9:283–291. [PubMed: 16429133]

Yonemoto W, McGlone ML, Taylor SS. N-myristylation of the catalytic subunit of cAMP-dependent protein kinase conveys structural stability. J Biol Chem. 1993; 268:2348–2352. [PubMed: 8428909]

Zhang J, Ma Y, Taylor SS, Tsien RY. Genetically encoded reporters of protein kinase A activity reveal impact of substrate tethering. Proc Natl Acad Sci U S A. 2001; 98:14997–15002. [PubMed: 11752448]

Zhang P, Ye F, Bastidas AC, Kornev AP, Wu J, Ginsberg MH, Taylor SS. An Isoform-Specific Myristylation Switch Targets Type II PKA Holoenzymes to Membranes. Structure. 2015; 23:1563–1572. [PubMed: 26278174]

Zheng J, Knighton DR, Xuong NH, Taylor SS, Sowadski JM, Ten Eyck LF. Crystal structures of the myristylated catalytic subunit of cAMP-dependent protein kinase reveal open and closed conformations. Protein Sci. 1993; 2:1559–1573. [PubMed: 8251932]

Zhong H, Sia GM, Sato TR, Gray NW, Mao T, Khuchua Z, Huganir RL, Svoboda K. Subcellular dynamics of type II PKA in neurons. Neuron. 2009; 62:363–374. [PubMed: 19447092]

Zhou J, Adams JA. Participation of ADP dissociation in the rate-determining step in cAMP-dependent protein kinase. Biochemistry. 1997; 36:15733–15738. [PubMed: 9398302]

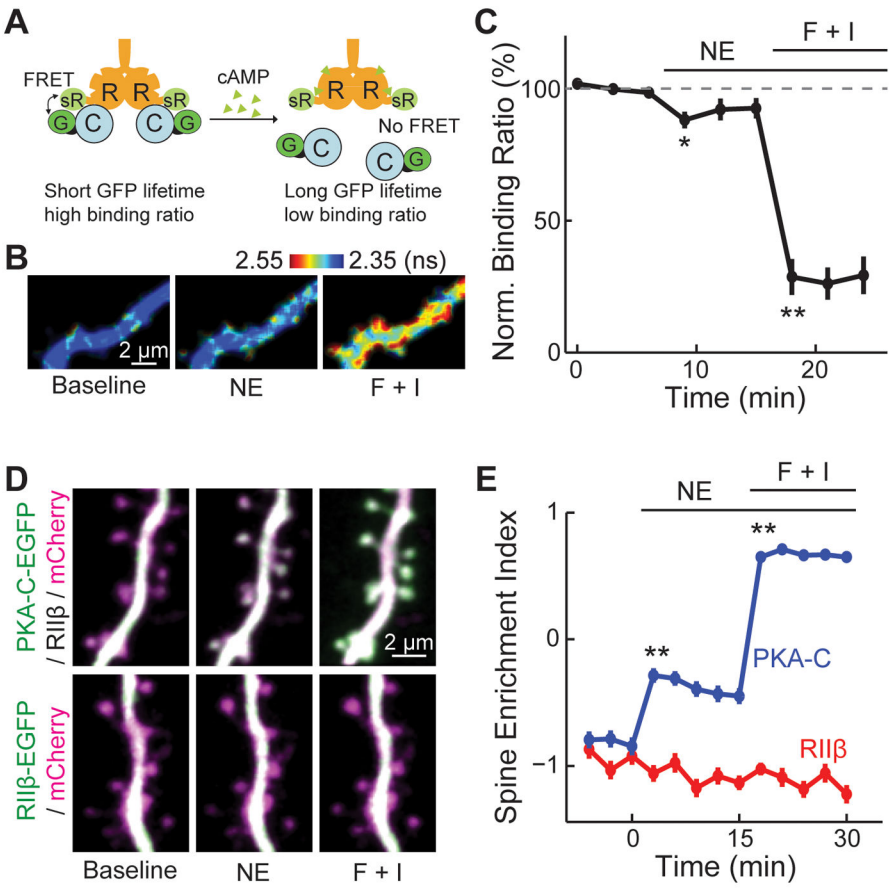

Figure 1. A fraction of PKA-C dissociated from PKA-R upon activation

(A) Schematic of the FRET/FLIM based measurement of PKA dissociation. R: PKA-RIIβ, C: PKA-C, G: GFP and sR: sREACh. (B, C) Representative 2pFLIM images and quantification of PKA dissociation in the presence of norepinephrine (NE) or forskolin and IBMX (F + I). n = 8 cells. (D, E) Representative images and quantifications of PKA-C-EGFP and PKA-RIIβ-EGFP localizations in the dendrites of CA1 neurons in cultured hippocampal slices. The red cytosolic marker mCherry was co-expressed to reveal the neuronal morphology. n = 69/11 (spines/cells) for PKA-C, and 25/6 for PKA-RIIβ. See also Figure S1 and S2.

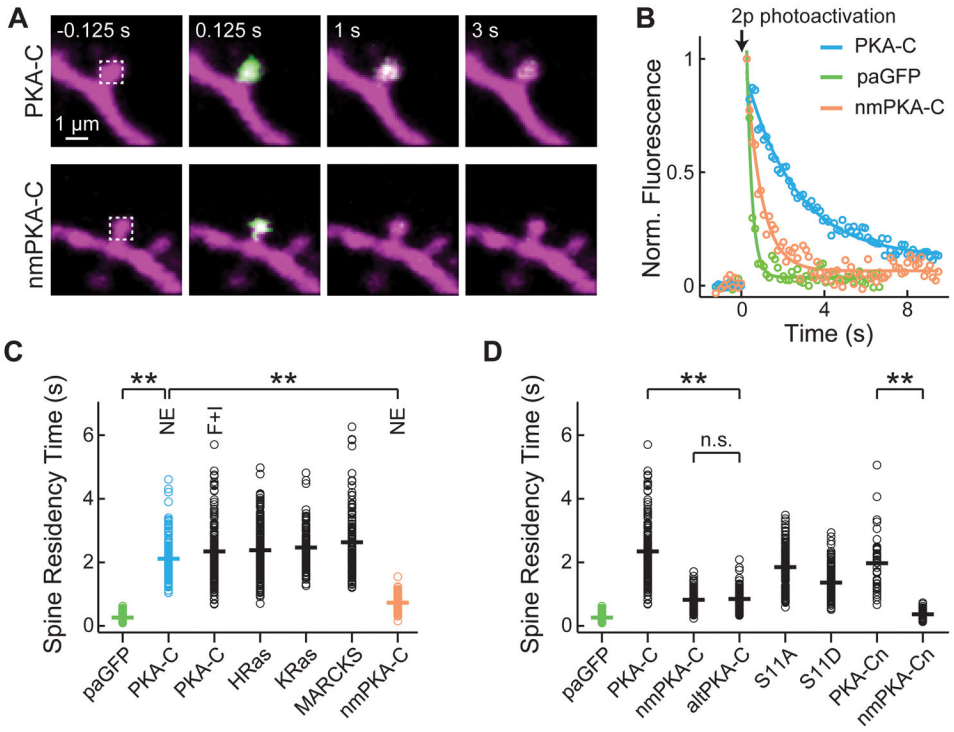

Figure 2. Activated PKA-C moved more slowly than a cytosolic protein via its N-terminal myristoylation

(A) Representative image series of two-photon mediated photoactivation experiments of wildtype and non-myristoylated (nm) PKA-C fused to paGFP, as shown in green, in dendritic spines of CA1 neurons. Untagged PKA-RIIβ and mCherry were co-expressed. 20 μM norepinephrine was bath applied to activate PKA. paGFP was photoactivated at time zero nearly instantaneously at the spine head (white dash box). (B) Representative fluorescence decay curves for spines expressing the indicated constructs in the presence of norepinephrine. (C) Collective data of the spine residence times for the indicated constructs. Where indicated, norepinephrine or forskolin and IBMX was added. The colors correspond to those in panel B. n = 193/10 (spines/cells) for paGFP; 148/9 for PKA-C with norepinephrine; 157/8 for PKA-C with forskolin and IBMX; 208/11 for HRas; 99/5 for KRas; 126/7 for MARCKS; 96/11 for nmPKA-C with norepinephrine. (D) Analysis of determinants of PKA-C diffusion. Forskolin and IBMX were added where stimulation of PKA is needed. n = 111/5 (spines/cells) for nmPKA-C; 100/7 for altPKA-C; 161/8 for PKA-C-S11A (S11A); 136/7 for PKA-C-S11D (S11D); 40/4 for PKA-Cn; and 50/5 for nmPKA-Cn. See also Figure S3.

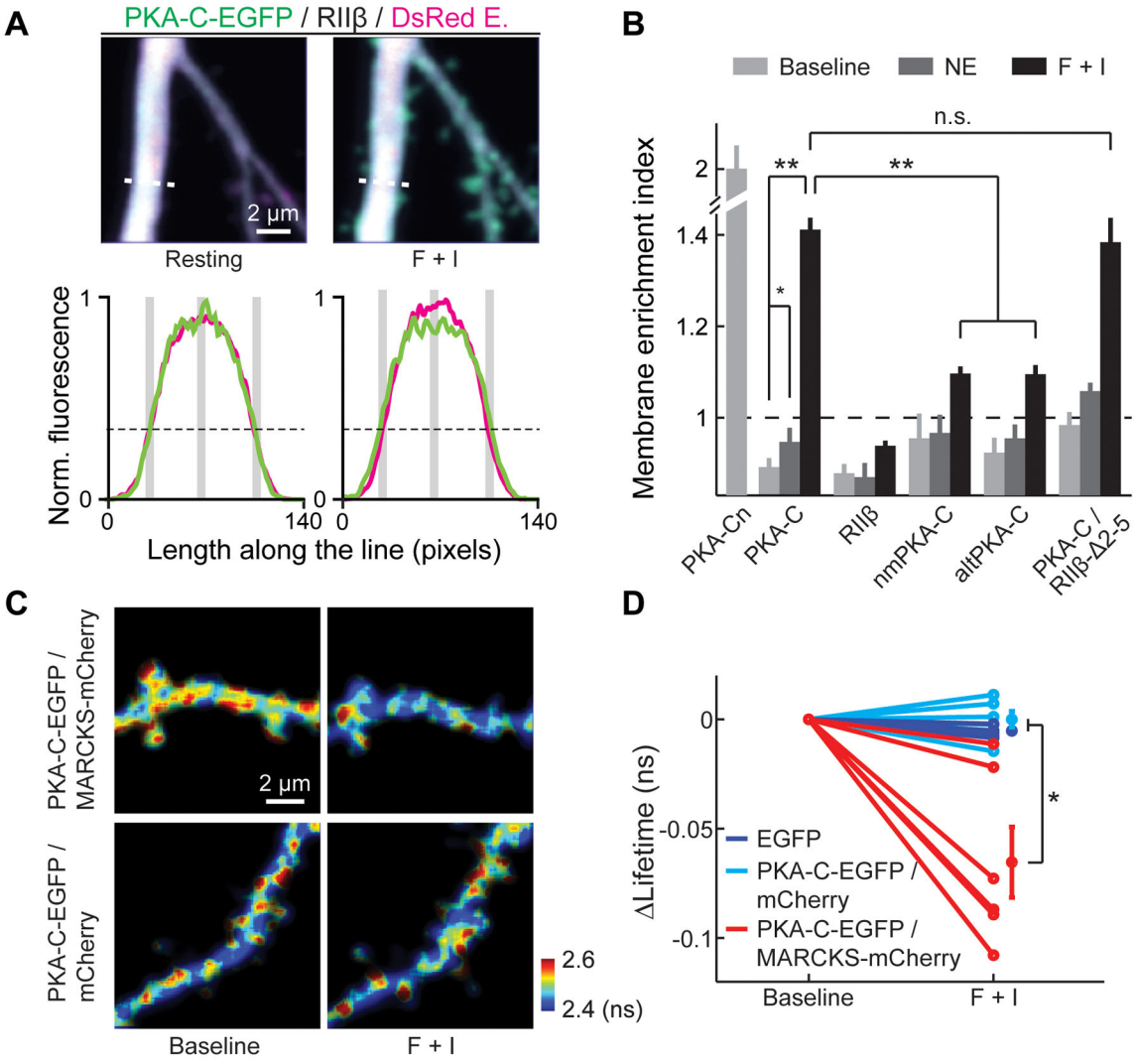

Figure 3. N-terminal myristoylation targeted PKA-C to the plasma membrane in neurons

(A) Top, representative single z-plane images of wildtype PKA-C distributions at rest and after stimulation by forskolin and IBMX in the primary apical dendrite of a CA1 neuron. Bottom, fluorescence line profiles along the white dashed lines in the top images for PKA-C (green) and the cytosol marker (red). The black dashed lines mark 30% of the maximum red fluorescence. The gray bars indicate the positions of measurements. (B) Averaged MEIs for the indicated constructs before and after stimulation. n = 8 cells for PKA-Cn, 11 for PKA-C, 6 for PKA-RIIβ, 6 for nmPKA-C, 6 for altPKA-C, 5 for PKA-C co-expressed with PKA-RIIβ-Δ2–5. Statistical significance was tested using the Wilcoxon signed rank test as the data were linked within each group. (C, D) Representative 2pFLIM images (C) and baseline-subtracted EGFP lifetimes (D) of hippocampal pyramidal neurons expressing the indicated FRET donor-acceptor combination at the baseline and stimulated conditions. See also Figure S4, S5 and S6.

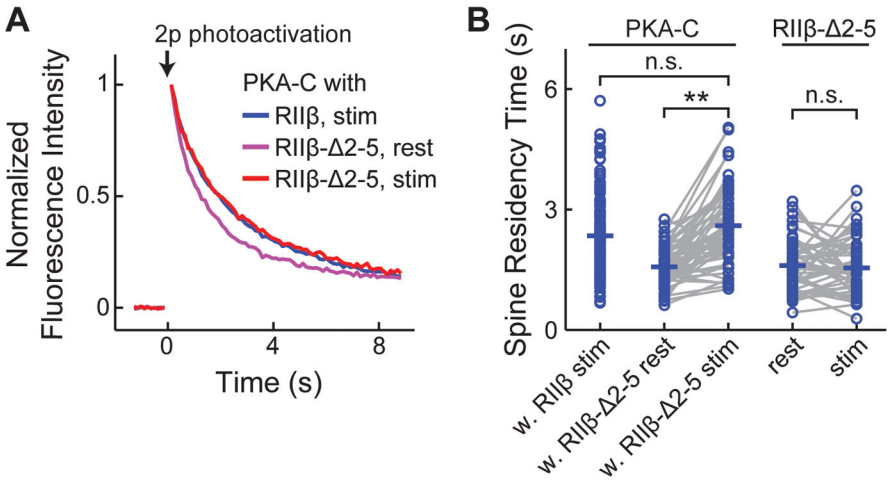

Figure 4. The low mobility of PKA-C did not require AKAP binding

(A, B) Averaged fluorescence decay curves (A) and spine-residence times (B) for the indicated construct combinations before and after forskolin/IBMX stimulation. The data for PKA-C-paGFP/RIIβ after stimulation is same as that in Figure 1. n = (spines/cells) 57/8 for PKA-C-paGFP/RIIβ-Δ2–5; and 51/9 for RIIβ-Δ2–5-paGFP.

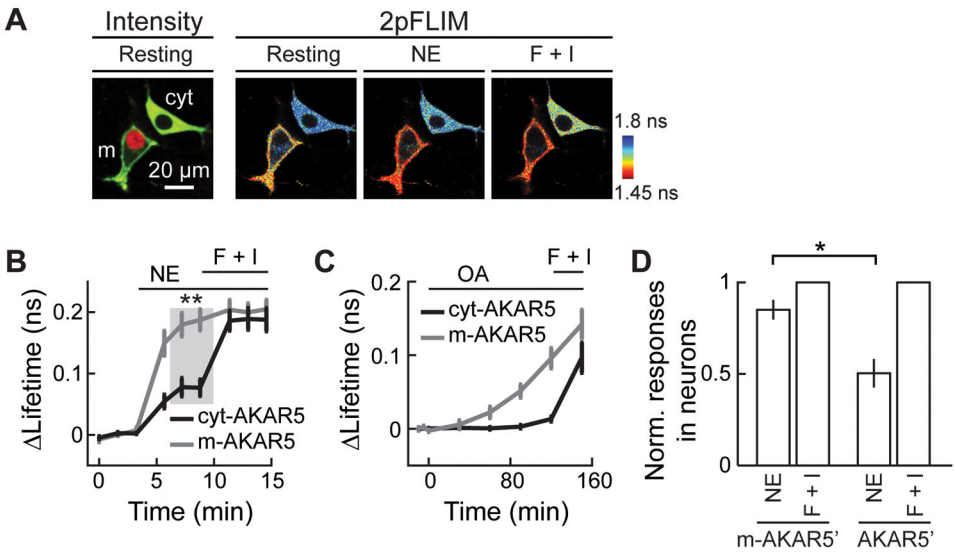

Figure 5. Membrane associated AKAR5 exhibited higher sensitivity than cytosol AKAR5 to stimulations of endogenous PKA activity

(A) Representative two-photon fluorescence intensity image (left) and 2pFLIM image series (right) of HEK 293 cells expressing either cyt-AKAR5 alone or co-expressing mAKAR5 with mCherry-histone2b. (B) Collective lifetime changes of m-AKAR5 and cyt-AKAR5 in response to 0.1 μM norepinephrine followed by forskolin and IBMX. n = 13 for m-AKAR5 and 9 for cyt-AKAR5. (C) Lifetime responses of cyt-AKAR5 and m-AKAR5 to treatment with 100 nM okadaic acid (OA) followed by forskolin and IBMX. n = 20 each. (D) Lifetime changes of AKAR5′ and m-AKAR5′ in neurons in response to 0.3 μM norepinephrine normalized to maximal responses induced by forskolin and IBMX. n = 5 for both constructs.

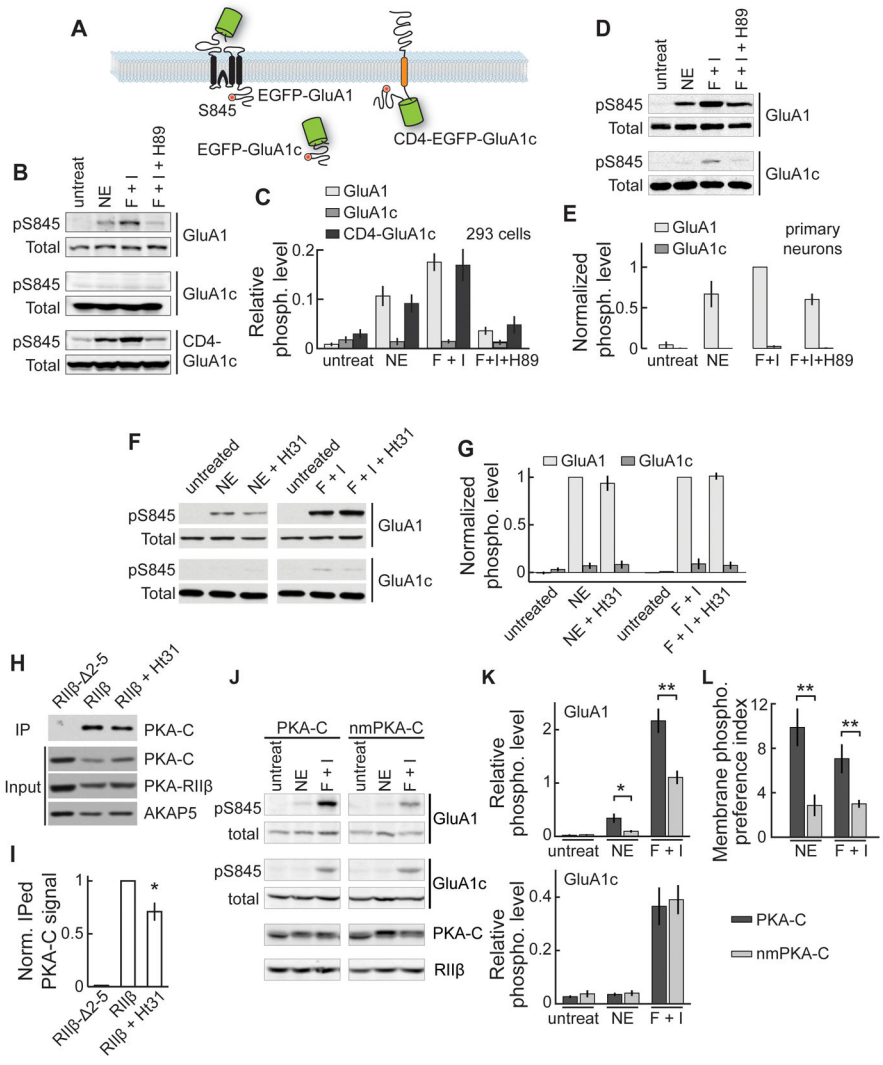

Figure 6. PKA preferentially phosphorylated a membrane bound substrate in an AKAP-independent and myristoylation-dependent manner

(A) Schematic illustrations of the substrate constructs. (B, C) Representative western blots (B) and quantifications (C) of S845 phosphorylation of the indicated constructs in HEK cells, which underwent the indicated stimulations. n = 5 independent experiments for EGFP-GluA1, 4 for EGFP-GluA1c, and 5 for CD4-EGFP-GluA1c. (D, E) Representative western blots and collective results for S845 phosphorylation of GluA1 and GluA1c carried out in primary rat cortical neuronal cultures. (F, G) Representative western blots and collective results of S845 phosphorylation of the indicated constructs in HEK cells, which underwent the indicated stimulations, with or without pre-incubation with St-Ht31. n = 5 for norepinephrine, and 4 for F + I. (H, I) Representative western blots and collective results of co-IP experiments with or without St-Ht31 treatment. PKA-C and AKAP5 were co-expressed with wildtype or mutant PKA-RIIβ as indicated. n = 4. (J) Representative western blots from HEK293 cells expressing PKA-RIIβ, EGFP-GluA1 and EGFP-GluA1c together with wildtype PKA-C or nmPKA-C treated with 1 μM NE or forskolin/IBMX as indicated.

(K) Collective results of the relative phosphorylation levels for GluA1 (top) and GluA1c (bottom). n = 6. (L) MPPIs for wildtype PKA-C and nmPKA-C across different treatment conditions.

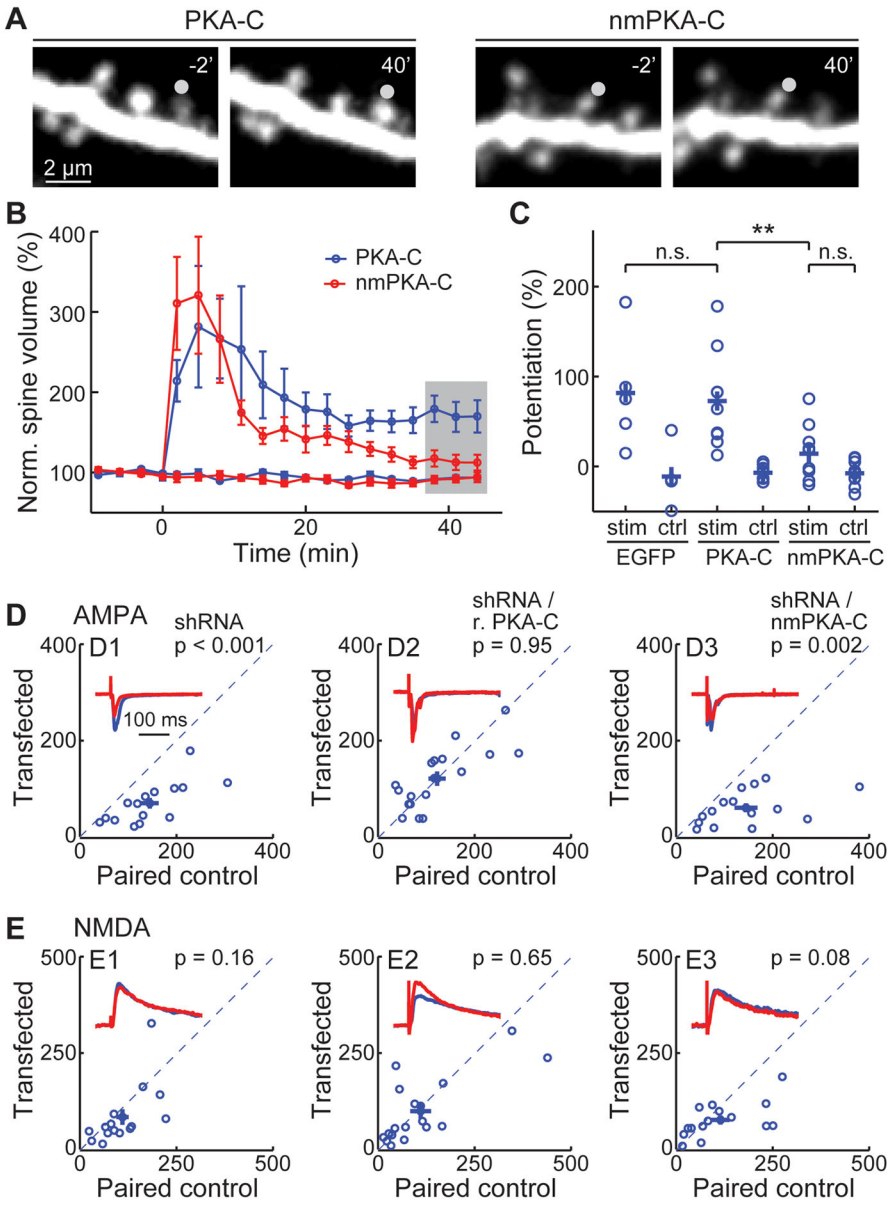

Figure 7. The N-terminal myristoylation of PKA-C is required for supporting normal synaptic plasticity

(A) Representative images, (B) collective time courses, and (C) the degree of lasting potentiation, as measured at the shaded time points in panel B. The gray circles in panel A indicates the uncaging position. Neurons were transfected with EGFP, PKA-C-EGFP/RIIβ/mCherry or nmPKA-C-EGFP/RIIβ/mCherry as indicated. (D, E) Representative traces (red) normalized to the control (blue) and scatter plots of paired AMPA (D) and NMDA (E) currents from neighboring untransfected CA1 neurons paired with those transfected with sh-PKA-C (labeled as shRNA) and the indicated shRNA-resistant rescuing constructs. Statistical significance was tested using a paired t-test. See also Figure S7.